Title

La-doped SrTiO3 films with large cryogenic thermoelectric power factors

Journal

Applied Physics Letters, 102(18)

Authors

Cain, Tyler A
Kajdos, Adam P
Stemmer, Susanne

Publication Date

2013-05-06

Peer reviewed

La-doped $SrTiO_3$ films with large cryogenic thermoelectric power factors

Tyler A. Cain, Adam P. Kajdos, and Susanne Stemmer[a)]
Materials Department, University of California, Santa Barbara, California 93106-5050, USA

(Received 13 March 2013; accepted 21 April 2013; published online 6 May 2013)

The thermoelectric properties at temperatures between 10 K and 300 K of La-doped $SrTiO_3$ thin films grown by hybrid molecular beam epitaxy (MBE) on undoped $SrTiO_3$ substrates are reported. Below 50 K, the Seebeck coefficients exhibit very large magnitudes due to the influence of phonon drag. Combined with high carrier mobilities, exceeding 50 000 $cm^2\ V^{-1}\ s^{-1}$ at 2 K for the films with the lowest carrier densities, this leads to thermoelectric power factors as high as 470 $\mu W cm^{-1} K^{-2}$. The results are compared with other promising low temperature thermoelectric materials and discussed in the context of coupling with phonons in the undoped substrate. © *2013 AIP Publishing LLC*. [http://dx.doi.org/10.1063/1.4804182]

Oxide materials have recently generated renewed attention as promising high-temperature thermoelectric materials due to relatively high thermoelectric figures of merit and other advantages, such as chemical stability and more earth-abundant constituents.[1–8] Doped $SrTiO_3$ exhibits a large increase in electron mobility at low temperatures.[9,10] In combination with its large Seebeck coefficient (S),[2,7,11] this makes doped $SrTiO_3$ potentially useful for thermoelectric cooling applications to cryogenic temperatures. Thermoelectric coolers at cryogenic temperatures are of great interest for applications such as superconducting electronics and infrared detectors. The maximum temperature difference of a thermoelectric cooling device is $\frac{1}{2}\ ZT^2$, where T is the temperature and the dimensionless thermoelectric figure-of-merit is ZT. Thus, efficient cooling requires large ZT, defined as $[(S^2\sigma)/\kappa]T$, where σ is the electrical conductivity and κ the thermal conductivity. The diffusive Seebeck coefficient rapidly approaches zero as the temperature nears 0 K, dramatically reducing the thermoelectric power factor ($S^2\sigma$) of most materials. At low temperatures, the influence of phonon drag can serve to increase the magnitude of the Seebeck coefficient.[12–14] The magnitude of the phonon drag contribution to the Seebeck coefficient depends strongly on the temperature and dopant/defect density of the material. Bulk $SrTiO_3$ single crystals exhibit phonon drag at low temperatures.[2] Characterizing the intrinsic thermoelectric properties of $SrTiO_3$ at low doping levels can be challenging due to defects that trap carriers.[15]

Here we report on the thermoelectric properties of $SrTiO_3$ grown by hybrid molecular beam epitaxy (MBE)[16] and doped with La to achieve a wide range of carrier densities, between $2 \times 10^{20}\ cm^{-3}$ and $8 \times 10^{17}\ cm^{-3}$. The samples with low carrier densities in this series allow for the study of phonon drag. We show that the hybrid MBE films exhibit electron mobilities greater than 50 000 $cm^2\ V^{-1}\ s^{-1}$ (at 2 K), exceeding those of bulk samples and previously reported films.[10] The combination of high electron mobilities and the phonon drag contribution to the Seebeck coefficient yields cryogenic power factors that exceed those of the best low temperature thermoelectric materials, such as $Bi_{1-x}Sb_x$ (Refs. 17 and 18).

Epitaxial $SrTiO_3$ films were grown on (001) $SrTiO_3$ substrates by hybrid MBE using substrate temperatures between 800 and 900 °C, measured by an optical pyrometer, as described elsewhere.[16,19] Lanthanum dopants were supplied by a solid effusion cell source operated at different temperatures to control the carrier concentrations in the $SrTiO_3$ thin films. All samples had an undoped $SrTiO_3$ buffer layer (of varying thickness, 30–300 nm) between the substrate and the La-doped film. Samples were annealed at 800 °C in 1 atm oxygen for 30 s to ensure oxygen stoichiometry. Temperature-dependent Hall, sheet resistance, thermal conductivity, and Seebeck measurements were performed using a Physical Properties Measurement System (Quantum Design). The Seebeck coefficients were corrected to account for the temperature dependent resistivity.[20] The required correction was less than 2% for all Seebeck coefficients reported here. Ohmic contacts were 40 nm Al/20 nm Ni/4000 nm Au, where the Al layer contacts the $SrTiO_3$, and deposited by electron beam evaporation. Hall and sheet resistance (R_S) measurements were carried out in van der Pauw geometries. A rectangular Hall bar ($4 \times 10\ mm^2$) was used for the in-plane Seebeck coefficient measurements. Film thicknesses used to calculate electrical conductivity and three-dimensional carrier densities were taken from the growth rate determined by the period of RHEED intensity oscillations. Film thicknesses ranged from ~160 nm to 1280 nm, with greater thicknesses needed to measure films with lower carrier concentrations due to the well-known surface depletion of $SrTiO_3$ (Refs. 21–23). The carrier concentration n was calculated under the assumption of conduction due to one carrier type as $n = 1/(t \cdot e \cdot R_H)$, where t is the thickness of the doped layer, e the electron charge, and R_H the measured 2D Hall coefficient. The Hall mobility μ_H was calculated as $\mu_H = R_H/R_S$. The Hall carrier density determined in this way varied up to ~28% with temperature, which was not systematic with carrier density or temperature. The conduction band structure consists of a light and a heavy electron band, whose degeneracy at Γ is lifted at temperatures below the cubic-to-tetragonal phase transformation (~105 K). At the carrier concentrations studied here, several bands may be occupied,[24] which can cause an apparent variation in carrier density with temperature, and may require the use of a correction in extracting the correct density from

[a)]Electronic mail: stemmer@mrl.ucsb.edu

the Hall coefficient.[25] La-dopant concentrations were measured previously using secondary ion mass spectrometry, and compared with the measured Hall density.[10] The discrepancy between the two measurements is less than 5% for carrier densities of $1 \times 10^{18}\,\mathrm{cm}^{-3}$ and below, and increases to about 30% for carrier densities in the low-to-mid $10^{19}\,\mathrm{cm}^{-3}$ (Ref. 10).

Figure 1 shows the temperature dependent Hall mobility of $SrTiO_3$ films with different carrier densities. At 300 K, the mobility is $\sim 7\,\mathrm{cm}^2\,\mathrm{V}^{-1}\,\mathrm{s}^{-2}$, independent of the carrier density, as it is dominated by phonon scattering.[9] At temperatures below 200 K, the Hall mobility becomes highly dependent on the La dopant concentration. It saturates at low temperatures for samples with the higher carrier densities, consistent with the mobility being limited by ionized impurity scattering from the La donor atoms. For the lowest doping concentration ($8.5 \times 10^{17}\,\mathrm{cm}^{-3}$), the mobility still increases with decreasing temperature, indicating that, for this sample, the mobility is still limited by phonon scattering. At 2 K, the Hall mobility of this sample is 53 200 $\mathrm{cm}^2\,\mathrm{V}^{-1}\,\mathrm{s}^{-2}$. The higher mobility of this sample compared to previous hybrid MBE grown $SrTiO_3$ (Ref. 10) is likely due to the higher growth temperature used here.

Figure 2(a) summarizes the electrical conductivity of the doped $SrTiO_3$ films. Around 300 K, the electrical conductivity increases proportionally with the carrier concentration, because of the constant electron mobility. At low temperatures (<20 K), a crossover occurs, in which films with higher mobility have higher conductivity than those with higher carrier densities. At these temperatures, the films with the highest conductivity are films that have slightly larger ($2 \times 10^{18}\,\mathrm{cm}^{-3}$ and $4 \times 10^{18}\,\mathrm{cm}^{-3}$, respectively) carrier densities than the film with the highest mobility.

Figure 2(b) shows the Seebeck coefficient, which is negative (n-type) for all dopant concentrations, and, as expected, scales with the carrier density. Samples with carrier concentrations below $10^{19}\,\mathrm{cm}^{-3}$ exhibit maxima in the absolute value of the Seebeck coefficient below 50 K, typical for phonon drag, which has been previously reported for undoped, bulk $SrTiO_3$ (Ref. 2). The temperature at which the Seebeck coefficient peaks is a function of the doping concentration. The peak due to phonon drag also becomes less pronounced at higher carrier concentrations relative to the diffusive component of the Seebeck coefficient. The carrier concentration dependence is known to be due to carriers being preferentially scattered by the ionized donors and by a saturation effect.[12]

The thermoelectric power factors are shown in Fig. 3. The power factor increases upon cooling from 300 K and peaks at a temperature (T_{max}). T_{max} increases with carrier concentration, except for the film with a carrier concentration of $8 \times 10^{17}\,\mathrm{cm}^{-3}$, which does not exhibit a downturn in power factor between 12 K and 300 K. The maximum power factor is $469\,\mu\mathrm{W cm}^{-1}\,\mathrm{K}^{-2}$ at $T_{max} = 15.5$ K for a carrier concentration of $1.95 \times 10^{18}\,\mathrm{cm}^{-2}$. For comparison,

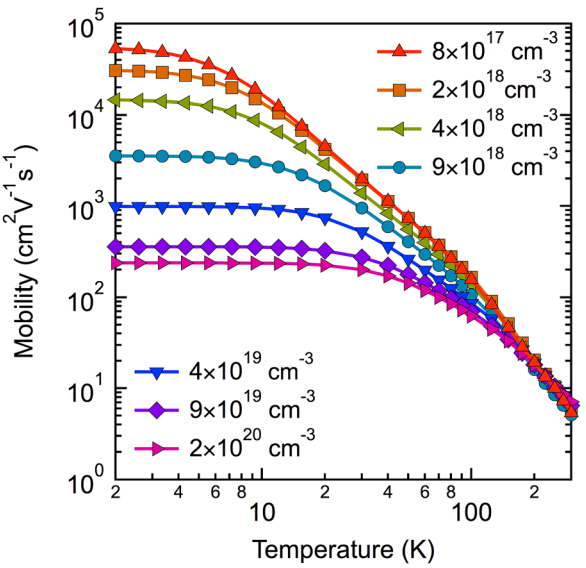

FIG. 1. Extracted Hall mobility as a function of temperature for La-doped $SrTiO_3$ thin films with carrier concentrations ranging between $8 \times 10^{17}\,\mathrm{cm}^{-3}$ and $2 \times 10^{20}\,\mathrm{cm}^{-3}$.

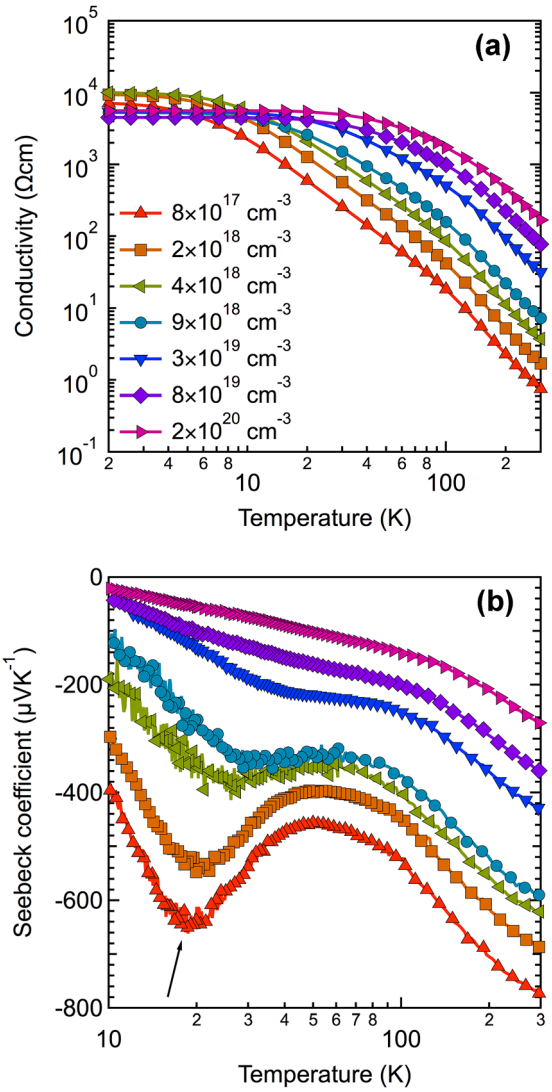

FIG. 2. (a) Electrical conductivity and (b) Seebeck coefficient as a function of temperature for La-doped $SrTiO_3$ thin films with different carrier concentrations on undoped $SrTiO_3$ substrates. For clarity, the symbols are only placed at every fifth data point recorded in the experiments. Note that the two graphs have different temperature axes scales. The arrow in (b) points to the phonon drag feature.

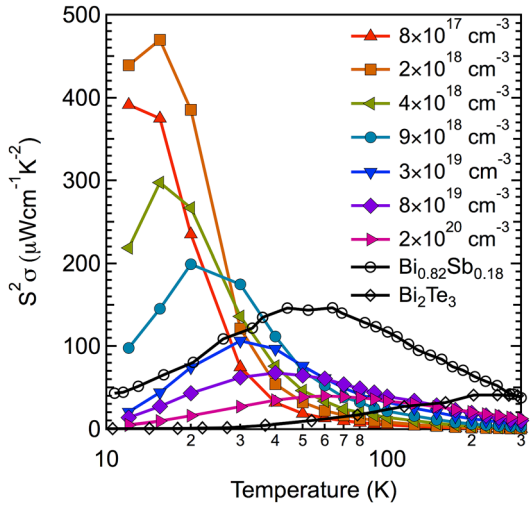

FIG. 3. Thermoelectric power factor, $S^2\sigma$, as a function of temperature for La-doped $SrTiO_3$ thin films with different carrier concentrations on undoped $SrTiO_3$ substrates. The power factors of $Bi_{0.82}Sb_{0.18}$ (Ref. 18) and Bi_2Te_3 (Ref. 26) are shown for comparison.

the power factors of Bi_2Te_3 (Ref. 26), a widely used commercial thermoelectric, and $Bi_{0.82}Sb_{0.18}$ (Ref. 18), which is the best low temperature thermoelectric, are also shown. Doped $SrTiO_3$ exhibits much larger power factors than Bi_2Te_3 at temperatures below 160 K for all carrier densities investigated here. $SrTiO_3$ films with carrier densities below $\sim 10^{19}$ cm^{-3} exhibit larger power factors than $Bi_{0.82}Sb_{0.18}$ at temperatures below 30 K. The maximum power factor of optimally doped $SrTiO_3$ at 15.5 K is more than three times larger than the maximum value for $Bi_{0.82}Sb_{0.18}$ (around 50 K).

While the electrical transport and diffusive component of the Seebeck component measured here represent those of the doped thin films, the phonon mean free path length (λ) at cryogenic temperatures is large. With $\lambda = 3\kappa/Cv_0$ (Ref. 27), where C is the heat capacity,[25] and v_0 is the phonon speed,[28] λ can be estimated to be several to tens of μm in the temperature range of interest here. Because of the long mean free path, the phonons in the $SrTiO_3$ substrate exchange momentum with the electrons in the doped film, thus influencing the observed phonon drag effect.[29] Thus, the low-temperature Seebeck coefficients, which are dominated by the phonon drag contribution, and the thermoelectric power factors must be considered to be that of the combined La-doped $SrTiO_3$ thin film/$SrTiO_3$ substrate system. It also means that the magnitude to the phonon drag effect will depend on the nature of sample's boundaries.[29]

Using the thermal conductivity of an undoped $SrTiO_3$ single crystal,[30] a maximum ZT of 0.046 is obtained at 15.5 K and a carrier concentration of 1.95×10^{18} cm^{-3}, which is larger than that of $Bi_{0.82}Sb_{0.18}$ at this temperature. The thermal conductivity of undoped $SrTiO_3$ exhibits a maximum (>20 Wm^{-1}K^{-1})[30] between 20 K and 30 K, near the temperature at which the phonon drag effect is the largest. The thermal conductivity at cryogenic temperatures will depend, to a large extent, on the sample's boundaries, making estimates of ZT using thin film data not relevant for any practical application.

In summary, we have demonstrated that doped-$SrTiO_3$-film/$SrTiO_3$-substrate structures grown by hybrid MBE achieve large power factors in excess of those of known good low temperature thermoelectric materials. The low defect and carrier concentrations achievable in hybrid MBE enable both high electron mobilities and large phonon drag contributions to the Seebeck coefficient. Large phonon mean-free paths at cryogenic temperatures allow for reducing the thermal conductivity through nanostructuring or superlattices,[31] but the effect of such approaches on the phonon drag component of the Seebeck coefficient must also be evaluated.

The authors acknowledge valuable discussions with David Cahill and support through the Center for Energy Efficient Materials, an Energy Frontier Research Center funded by the DOE (Award No. DESC0001009). T.A.C. received support from the Department of Defense through a NDSEG fellowship and A.P.K. from the National Science Foundation (NSF) through a Graduate Research Fellowship (Grant No. DGE-1144085). The work made use of the MRL Shared Experimental Facilities, which are supported by the MRSEC Program of the NSF under Award No. DMR-1121053. This work also made use of the UCSB Nanofabrication Facility, a part of the NSF-funded NNIN network.

[1]I. Terasaki, Y. Sasago, and K. Uchinokura, Phys. Rev. B **56**, R12685 (1997).
[2]T. Okuda, K. Nakanishi, S. Miyasaka, and Y. Tokura, Phys. Rev. B **63**, 113104 (2001).
[3]I. Matsubara, R. Funahashi, T. Takeuchi, S. Sodeoka, T. Shimizu, and K. Ueno, Appl. Phys. Lett. **78**, 3627 (2001).
[4]S. Ohta, T. Nomura, H. Ohta, M. Hirano, H. Hosono, and K. Koumoto, Appl. Phys. Lett. **87**, 092108 (2005).
[5]K. Koumoto, Y. Wang, R. Zhang, A. Kosuga, and R. Funahashi, Annu. Rev. Mater. Res. **40**, 363 (2010).
[6]J. He, Y. Liu, and R. Funahashi, J. Mater. Res. **26**, 1762 (2011).
[7]J. D. Baniecki, M. Ishii, H. Aso, K. Kurihara, and D. Ricinschi, J. Appl. Phys. **113**, 013701 (2013).
[8]S. Lee, G. Y. Yang, R. H. T. Wilke, S. Trolier-McKinstry, and C. A. Randall, Phys. Rev. B **79**, 134110 (2009).
[9]H. P. R. Frederikse and W. R. Hosler, Phys. Rev. **161**, 822 (1967).
[10]J. Son, P. Moetakef, B. Jalan, O. Bierwagen, N. J. Wright, R. Engel-Herbert, and S. Stemmer, Nature Mater. **9**, 482 (2010).
[11]B. Jalan and S. Stemmer, Appl. Phys. Lett. **97**, 042106 (2010).
[12]C. Herring, Phys. Rev. **96**, 1163 (1954).
[13]T. H. Geballe and G. W. Hull, Phys. Rev. **94**, 1134 (1954).
[14]A. R. Hutson, J. Phys. Chem. Solids **8**, 467 (1959).
[15]E. Ertekin, V. Srinivasan, J. Ravichandran, P. B. Rossen, W. Siemons, A. Majumdar, R. Ramesh, and J. C. Grossman, Phys. Rev. B **85**, 195460 (2012).
[16]B. Jalan, R. Engel-Herbert, N. J. Wright, and S. Stemmer, J. Vac. Sci. Technol. A **27**, 461 (2009).
[17]B. Lenoir, M. Cassart, J. P. Michenaud, H. Scherrer, and S. Scherrer, J. Phys. Chem. Solids **57**, 89 (1996).
[18]B. Lenoir, A. Dauscher, M. Cassart, Y. I. Ravich, and H. Scherrer, J. Phys. Chem. Solids **59**, 129 (1998).
[19]B. Jalan, P. Moetakef, and S. Stemmer, Appl. Phys. Lett. **95**, 032906 (2009).
[20]Quantum Design PPMS Application Note 1684-200, Rev. A0, 2012.
[21]Y. Aiura, I. Hase, H. Bando, T. Yasue, T. Saitoh, and D. S. Dessau, Surf. Sci. **515**, 61 (2002).
[22]A. Ohtomo and H. Y. Hwang, Appl. Phys. Lett. **84**, 1716 (2004).
[23]T. Hara, T. Ishiguro, and K. Shinozaki, Jpn. J. Appl. Phys., Part 1 **50**, 041502 (2011).
[24]H. Uwe, R. Yoshizaki, T. Sakudo, A. Izumi, and T. Uzumaki, Jpn. J. Appl. Phys., Part 1 **24**(Suppl. 24-2), 335 (1985), available at http://jjap.jsap.jp/link?JJAPS/24S2/335/.

[25]M. Ahrens, R. Merkle, B. Rahmati, and J. Maier, Physica B **393**, 239 (2007).
[26]V. A. Kulbachinskii, V. G. Kytin, A. A. Kudryashov, and P. M. Tarasov, J. Solid State Chem. **193**, 47 (2012).
[27]N. W. Ashcroft and N. D. Mermin, *Solid State Physics* (Brooks/Cole, Belmont, 1976).
[28]B. Hehlen, A.-L. Perou, E. Courtens, and R. Vacher, Phys. Rev. Lett. **75**, 2416 (1995).
[29]R. Fletcher, M. Diorio, A. S. Sachrajda, R. Stoner, C. T. Foxon, and J. J. Harris, Phys. Rev. B **37**, 3137 (1988).
[30]Y. Suemune, J. Phys. Soc. Jpn. **20**, 174 (1965).
[31]P. Pichanusakorn and P. Bandaru, Mater. Sci. Eng. R **67**, 19 (2010).